Internet of Things 19 (2022) 100552

Contents lists available at ScienceDirect

Internet of Things

journal homepage: www.elsevier.com/locate/iot

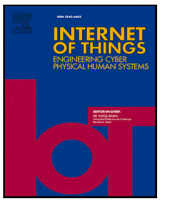

Research article

MagLoc: A magnetic induction based localization scheme for fresh food logistics

Amitangshu Pal [a,*], Krishna Kant [b]

[a] Computer Science and Engineering, Indian Institute of Technology Kanpur, Kanpur, India
[b] Computer and Information Sciences, Temple University, Philadelphia, PA, USA

ARTICLE INFO

Keywords:
Smart sensing
Industrial sensors
Food supply chain
Physical Internet
Magnetic communication
Localization

ABSTRACT

An IoT infrastructure to continuously monitor the fresh food supply chain can quickly detect food quality and contamination issues and thereby reduce costs and food wastage. This, in turn, involves several challenges including the development of inexpensive quality/contamination sensors to be deployed in a fine grain manner in the food boxes, technologies for sensor level communications, online data management and analytics, and logistics driven by such analytics. In this paper, we study the issues related to the communication among sensing modules deployed in the fresh food boxes and thereby an automated localization of the boxes that may have quality/contamination issues. In this context we study the near-field magnetic induction (NFMI) based communication and localization, as the ubiquitous RF communications suffer high attenuation through the water/mineral rich tissue media. An accurate localization of the sensors inside boxes within the food pallets is very challenging in this environment. In this paper we propose a novel magnetic induction based localization scheme, and show that with a small number of anchor nodes, the localization can be done without any errors for boxes as small as 0.5 meter on the side, and with small errors even for boxes half as big.

1. Introduction

Fresh food distribution and transportation is a huge and growing enterprise due to increasing consumption and expectations of "freshness" from the public. However, the fresh food transportation and distribution (T&D) suffers from dismal efficiency because of unplanned and uninformed distribution, which leads to substantial food spoilage and wastage. Furthermore, fresh food is also directly or indirectly responsible for a large number of food borne illnesses annually in the US and elsewhere. There is a recent move towards "physical Internet" [1] which attempts to bring some of the key attributes of Internet (resource/capacity sharing, standardized addressing, formats, and protocols, etc.) to distribution logistics. The physical Internet architecture is also extended for fresh food logistics to consider perishability/contamination centrally, devise mechanisms for their online sensing/communication, and exploit the information for intelligent, proactive distribution that enhances food freshness and safety, reduces food waste, increases T&D utilization and energy efficiency, and extends the sensor lifetimes as much as possible [2].

One of the key reasons of food wastage and loss in food logistics is the lack of quality related information (or shelf life of the products) during the distribution stage. Because of this, typical food logistics adopt First-In–First-Out (FIFO) distribution mechanism with the assumption that the oldest product has shorter shelf life. For example in Fig. 1(a) a FIFO distribution would have shipped pallets 1–4 based on the order of arrivals. However, a better distribution planning can be adopted if the accurate, online food qualities and known at the distribution end. An illustration of an intelligent, quality-aware distribution is shown in Fig. 1(b) where

* Corresponding author.
E-mail addresses: amitangshu@cse.iitk.ac.in (A. Pal), kkant@temple.edu (K. Kant).

https://doi.org/10.1016/j.iot.2022.100552
Received 24 November 2021; Received in revised form 4 April 2022; Accepted 19 May 2022
Available online 15 June 2022

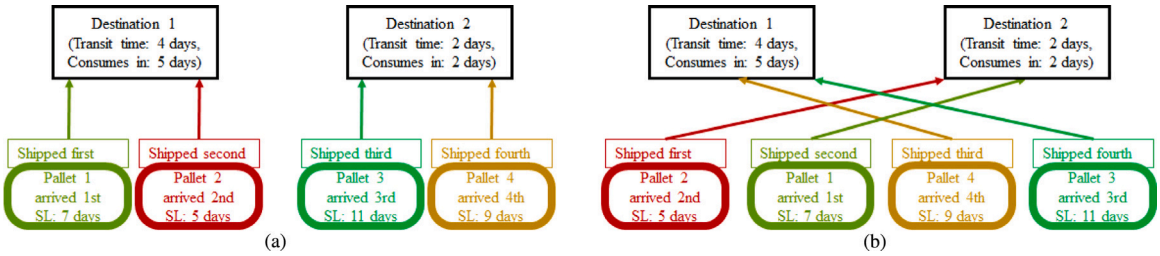

Fig. 1. Illustration of (a) FIFO vs (b) intelligent, quality aware pallet distribution in a food logistics. Here "SL" stands for shelf life. (a) A FIFO distribution ships pallets 1–4 according to their order of arrivals, based on the false assumption that the oldest pallets have the shortest shelf life and should be shipped first. However in reality destination 1 may take more transit time and have slower consumption rate, which may lead to quality loss and spoilage to the pallets 1 and 2. Therefore in an intelligent distribution, pallets 1 and 2 will be sent to destination 2 for faster consumption, whereas other pallets can be transported to destination 1 as they have higher shelf life. In this case all the pallets are consumed before their expiry.
Source: The figure is adapted from ChainLink Research (www.clresearch.com) [3].

the distribution orders are adjusted based on the shelf life of the pallets, along with their estimated transit and consumption time, which leads to successful delivery and consumption of the packages before their expiry. This simple example illustrates the necessity of an online quality/freshness monitoring of the packages in food logistics to reduce the extent of delivery wastage.

In this paper we develop food quality sensing and communication mechanisms for monitoring perishability/contamination in fresh food T&D pipeline, particularly during transport of food on carriers (e.g., trucks) or in warehouses. In particular, we explore mechanisms to automatically monitor, sense and communicate the fresh food quality as measured by appropriate sensors enclosed in the boxes that may be stored in a distribution center, warehouse or in transit in a truck, railcar, etc. This involves both the localization of the boxes containing sensor modules that detect quality/contamination issues and its communication to a local hub node. The communicated quality along with the positional identification of the boxes can be exploited to take proactive actions that can considerably improve the logistics efficiency, by reducing the food waste or triggering an early warning in case of a contamination.

Because of the high water content, RF signals degrade rapidly in these environments; therefore, we use the near-field magnetic induction (NFMI or simply MI) technology, which works quite well and provides adequate range for our application. NFMI communication works on the principle of resonant inductive coupling (RIC), which involves two matched coils, each forming a LC circuit with the same resonance frequency. RIC has been used successfully for extremely efficient power transfer over short distances and is used for contactless mobile charging, car battery charging, etc. NFMI communication modulates the magnetic field and forms the basis of near field communications (NFC) between mobile devices. NFMI communication has been studied in several earlier works, including our survey paper [4], therefore the focus of this paper is largely on its application in fresh food logistics. We demonstrate that the NFMI technology in the HF band (3–30 MHz) can be employed as a means of reliable communication in food logistics. To localize the sensors inside food boxes, we propose a novel magnetic induction based localization scheme, named MagLoc and study its accuracy via extensive simulations. The proposed MI based sensing and localization scheme can also be useful in similar RF challenged applications, including smart farming or aquatic agricultural monitoring.

The outline of the paper is as follows. Section 2 discusses the overall background and motivation of the research. Section 3 describes the suitability of MI communications and a brief overview of its channel modeling. Section 4 formulates the localization problem for locating the sensing devices. In this section we show that the localization problem is NP-hard, and present a heuristic approach. Section 5 shows extensive simulation and experimental results to explore the effectiveness of the mechanism. Related works are summarized in Section 6. The paper is concluded in Section 7.

2. Motivation and background

2.1. Emerging technologies for fresh food supply chain

Transportation and distribution of fresh food is a huge and growing enterprise due to both world wide sourcing of products and increasing recognition of the benefits of fresh fruit/vegetable dominated diets. Fresh food includes a large spectrum of products including raw and prepared (but not preserved) fruits, vegetables, fungii, dairy, seafood, meats, etc, with varying perishability characteristics and handling requirements. There are also increasing expectations of "freshness" from the public, which conflict with the goals of reducing food waste and its enormous environmental impact and cost. In the US, up to 40% of all food (and up to 50% of fresh food) is wasted resulting in $165 Billion annual cost [5], which in turn wastes fresh water resources, fertilizers, transportation/storage capacity, etc. Although the supply chain only accounts for only about 12% of the food waste directly, the indirect waste (due to retailers/customers throwing away food that spoils early or simply does not look good) is much higher [6]. The fresh food supply chain remains extremely inefficient, with only about 10%–20% of the carrying capacity used effectively [1].

These issues are being tackled on multiple fronts. One is the increasing deployment of so called 3rd party logistics (3PL) which allows a 3rd party to collectively serve the logistics needs of multiple customers and thereby wring out significant inefficiencies [7]. Several variants of the idea such as multiple companies sharing their delivery capacity without involving a third party are on the rise. Another significant development is the borrowing of ideas from Internet to create what is known as "Physical Internet" that includes

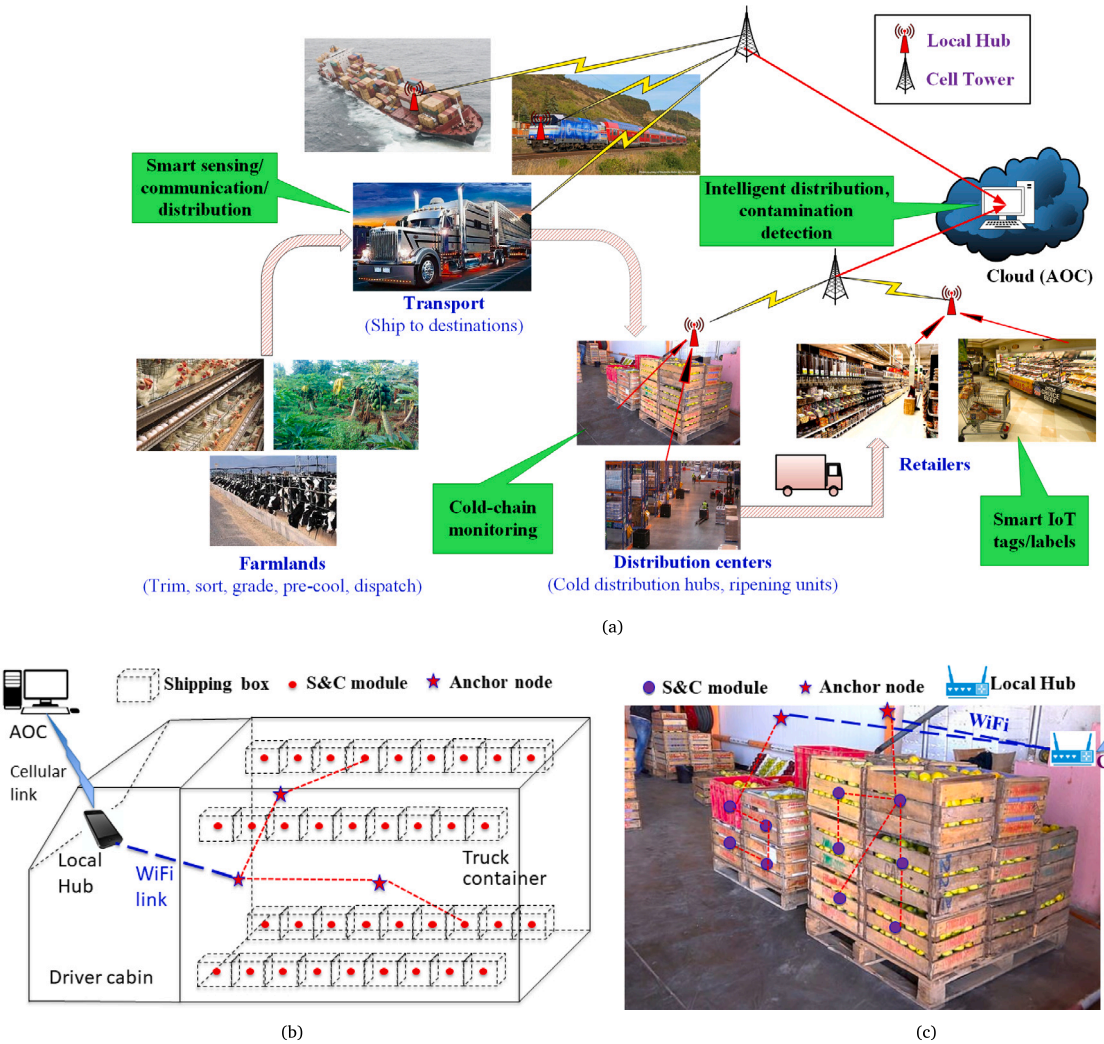

Fig. 2. (a) A smart and informed fresh food logistics. Communication infrastructure (b) inside a truck and (c) within a warehouse. In this figure, AOC denotes Analytics & Operations Center. These figures have been adapted from multiple sources that are either free or supported by creative commons licences.

modularized containers, standardized addressing mechanisms, automated operations (e.g., packing/unpacking, loading/unloading, sorting, positioning, etc.), and shared (rather than privately operated) logistics operations [1]. In the past, we have proposed the Fresh Food Physical Internet (FFPI or $F^2\pi$) to better integrate perishability into the physical internet [8]. Alongside, the developments in IoT technologies enable comprehensive automated monitoring and decision making. It is this last aspect that the we shall focus upon in this paper. Fig. 2(a) shows the conceptual view of the intelligent supply chain with all major components of the logistics providing data to and being driven by comprehensive analytics of this data in a cloud.

2.2. Sensing and communications for fresh food supply chain

Given the increasing availability of inexpensive IOT devices with sensing and communications capabilities, it is possible to deploy them densely for on-line monitoring of quality and contamination throughout the supply chain. This can play a central role in reducing waste, increasing efficiency, and enhancing food safety [11,12]. Our vision is that all boxes carrying perishable products will have one sensing node that detects crucial aspects of product quality including bacterial content, contamination etc. Recently a significant amount of research efforts are going on to develop such cheap food sensors, such as C_2Sense [13], FoodScan [14], Salmonella Sensing System [15] etc. Table 1 summarizes some of these food sensors. Although many such sensors currently under development target the end-customer (i.e., intended to be deployed in small retain packages that the retail customer can check during purchase and while the product is in the refrigerator), our goal is its deployment in the supply chain which has different deployment and usage requirements as discussed below.

Table 1
Different sensor types.
Source: Data obtained from [9,10].

Trade name/Biosensor	Organization
Time Temperature Indicator (TTI)	
Fresh-check	Temptime Corp.
Timestrip	Timestrip Plc
OnVu	Ciba Specialty Chemical and Freshpoint
MonitorMark	3M™, Minnesota
Tempix	TEMPIX
FreshTag	Vitsab
Indicator sensors	
SensorQ	DSM NV
RipeSense	RipSense™
RediRipe	University of Arizona
Contamination sensors	
C_2Sense	C2Sense, Inc.
FoodScan	MS Tech
Salmonella Sensing System	Auburn University
Escherichia coli 0157:H7 in lettuce	MIT
Escherichia coli O157:H7 and Salmonella in meat	Michigan State University
Salmonella and Campylobacter in pork industry	Georgia Research Tech Institute
Staphylococcal enterotoxin B and Botuminum toxin A in tomatoes, sweet corn, beans and mushrooms	Naval Research Laboratory
Escherichia coli 0157, Salmonella, Listeria and Campylobacter	Molecular Circuitry Inc.

The supply chain largely deals with moving and storing "pallets" or large packages consisting of rectangular arrangement of smaller retail level boxes that in turn contain end-customer level packages. For example, a retail box may contain 20 individual packages of chicken that the end customer buys. For supply chain monitoring, it is enough if each retail box contains only one sensor; in case of a contact sensor, this sensor must be deployed in one of the customer packages inside the retail box, but other types of sensors (e.g., gas emission sensors) may not need any physical contact. A pallet might consist of $5 \times 5 \times 5$ arrangement of retail boxes, and we assume by default that every box has a sensor. Since the packaging and palletization is increasingly done by robotic mechanisms, it is possible to systematically insert one sensor per retail box in roughly the same position. However, while the pallets are in the supply chain, it should be possible to read these sensors via wireless means. That is, each sensor is really a sensing and communications (S&C) module with a suitable radio technology that can work through the media of fresh food, such as NFMI.

We envision these local, short range communications to further connect to longer range communications so that the data can eventually be deposited in a central place such as a cloud. However, in addition to communicating the quality data, we also need to associate the reported data to the position of the reporting box. Such a correlation can be very useful as described later. Thus the key problem addressed in this paper is localization of the sensors (or rather the boxes containing the sensors) under NFMI communications. We believe that this is the first work on localization using NFMI in this challenging environment.

Our vision is to deploy the sensing and communications (S&C) modules throughout the supply chain so that most, if not all, fresh food pallets in the supply chain carry them from source (where the pallets are initially prepared) until the destination (e.g., points of depalletization and retail distribution). This means that the pallets will be monitored while being transported by any means (e.g., truck, railcar, boat, etc.) or stored in a warehouse. In order to monitor the quality continuously, we need to deploy some sink radio modules on the carriers and in warehouse rooms so that they can communicated with the S&C modules in the pallets. All of these radios use the same technology, which we will largely consider as NFMI. Fig. 2(b) shows the overall architecture of the proposed system within a truck carrying one or more pallets of boxes with one S&C modules per box. The sink (or anchor) nodes are mounted on (or close to) the inner walls of the carrier; these nodes are equipped with both MI and WiFi interfaces. These nodes can easily connect with a local hub such as the WiFi access point or smartphone and from there connect to the central Analytics & Operations Center (AOC) that resides in the cloud for further analytics and action. Similar deployment happens in a cold-storage warehouse room as well, which is shown in Fig. 2(c).

2.3. Role of localization in smart fresh food supply chain

Given the centralized availability of the quality/contamination data in the AOC, it is possible to do deep analytics and drive a variety of decisions for reducing waste and enhancing the efficiency of the logistics. One important use of the information is the proactive early distribution of the pallets that are experiencing quality issues. That is, instead of carriers following the predefined delivery schedule and delivery points, the delivery destinations, schedules, and routes are altered (to the extent possible) so that the transit time of pallets with quality issues is reduced (at the cost of delaying others). This relates to the notion of "lateral distribution", i.e., distribution center to distribution center or even retailer to retailer distribution to reduce further quality loss and food wastage.

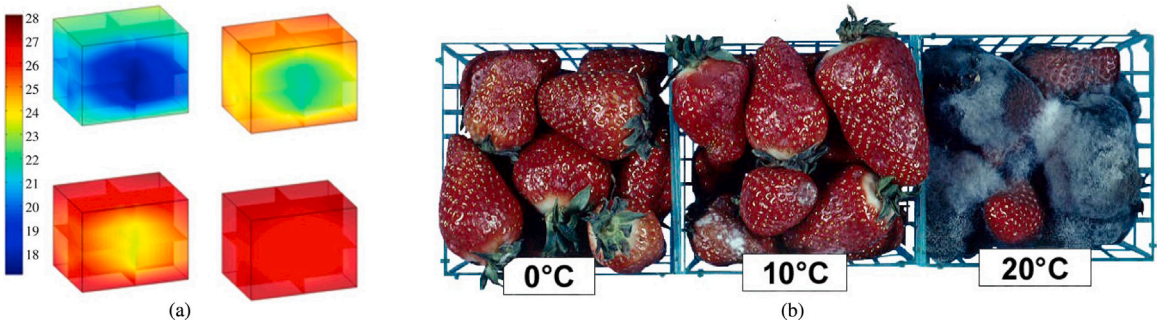

(a) (b)

Fig. 3. (a) Temperature variation inside a pallet as the container temperature increases from top-left to bottom-right (reprinted with permission from [16]). (b) The quality degradation of strawberries after 1 week of storage (reprinted with permission from [21], Photo Credit: Don Edwards, UC Davis).

With more significant quality loss, the product can often be directed to local food kitchens or sold to low end retailers in the area. These actions can be further modified based on other factors such as weather, warehouse space availability, endpoint needs, contractual flexibility, etc. More aggressive actions include adjustment of cooling in the carriers and warehouses to minimize their energy consumption so as to maintain quality degradation within the acceptable bounds. Finally, if the contamination is detected or there are signs of significant degradation, the product can be removed from the distribution pipeline so that its carbon footprint and potential ill effects can be minimized. The analytics required to take these actions could be quite sophisticated and is crucially dependent on timely quality/contamination information.

All of the actions above relate to entire pallets since they are not opened until the stage of local distribution. Thus simply knowing how many boxes within a pallet have quality issue may be adequate — the identification of the corresponding boxes is not needed. However, the localization, even if done approximately, can be useful in several respects as described below.

The most crucial use is in the analytics itself. The reason is that the temperature and other parameters inside a pallet vary from box to box depending on their positions. This is shown in Fig. 3(a) where the temperature variation of 45 packages inside a pallet was recorded over a period of 24 h [16]. As expected, the rate of temperature increase at the core of the pallet is lower than that of outside. This temperature variation results in a wide variation in food quality, although the extent of this variation depends on the food types. Fig. 3(b) shows the quality degradation of strawberries kept at three different temperatures over a period of one week. After one week the strawberries stored at 0 °C remains fresh, while those of 20 °C spoiled completely. Thus knowing the box position within the container can provide much more granular data and hence better analytics of the state of the pallet and how to improve the logistics in the future.

Another reason for tracking box positions is that it helps immediate discarding or return of boxes with quality/contamination issues at the point of depalletization. Without it, such boxes will be delivered to the retailer who then must inspect the contents and take further action. Yet another reason is the more effective cooling management. If the position of the box reporting temperature or quality issue is known, it is easier to conclude if the issue is related to cooling control or something else (e.g., precooling effectiveness, starting quality, etc.) and this knowledge can be used to optimize cooling.

3. Wireless communication through food media

In this section we review some wireless communication technologies and argue that the NFMI technology is best suited for the application. We also briefly review the channel modeling for this technology.

3.1. RF vs. Ultrasound vs. NFMI

Because of their ubiquity, short-range RF based communication such as BlueTooth Low Energy (BLE) would be a natural choice for our application; unfortunately, RF is known to suffer high signal absorption in aqueous/tissue media of fresh food [17]. For example in [18] the authors have shown that in tissue medium, the path loss at 0.5 m distance is 47–49 dB at 403.5 MHz. Similar studies [19,20] have also reported that the attenuation values in tissue medium ranges from 20 dB at 100 MHz to 60 dB at 1 GHz for distances less than 10 cm. Although the use of lower frequencies help reducing absorption, this will need bigger antennas and will cause severe interference in a dense environment consisting of multiple boxes each having some sensing units.

Ultrasonic communication can work in aqueous and tissue medium; however, such communication is deeply affected by multipath fading [22] due to the inhomogeneity of the tissue medium, presence of small organs, particles etc. which affects the sound velocity. This makes the detection and decoding of the signal challenging at the receiver, due to numerous attenuated and delayed versions of the same transmitted signal. Another issue of ultrasonic communication is that a significant portion of the energy is absorbed (although lower then RF) and converted into heat when ultrasounds propagate, which leads to temperature increase and thus quality loss of perishable products.

Compared to RF and Ultrasound, NFMI suffers from negligible signal fluctuations and multi-path effects, which are advantageous for localization [23]. Along with these characteristics, the ability to use small coils (2.5/5.0 cm in our experiments), short

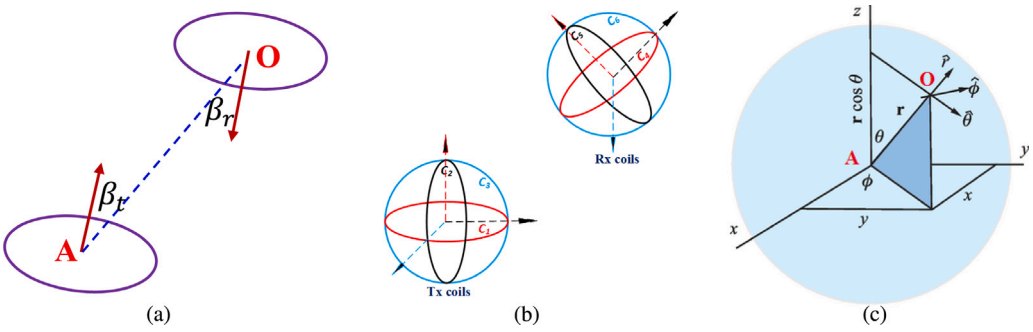

Fig. 4. (a) The intersection angle between two unidirectional coils. (b) Illustration of two tri-directional coils. The arrows are showing the unit normal vectors, perpendicular to the coil planes. (c) Spherical coordinate system where A and O are the positions of the transmitter and receiver respectively.

transmission range (e.g., 1.5 m), and a decent data rate (e.g., 596 Kb/s) makes NFMI suitable for our application. *Apart from these, ultra-low-power MI solutions also consume less power than RF and ultrasound over short distances.* MI chipset may draw as little as 7 mA for voice and data communication over a 1 m link, whereas RF systems require 10 times of this amount [24]. The reasons for such low-power consumption are as follows. First, is the ability of MI communication in the carrier frequency of 11–15 MHz, which offers tremendous advantages over 2.4 GHz RF system. For example, an on-chip amplifier operating at 2.4 GHz consumes several mA current, whereas an 11.5 MHz amplifier consumes only few hundreds of μAs [24]. Similar current savings are observed on other blocks of the transceivers. The RF systems also require more complex and power-hungry processors as compared to MI. Finally, the high-frequency RF systems may need higher power semiconductor processes such as silicon germanium (SiGe) or BiCMOS.

Acoustic transceivers are typically designed for long distance communication, with higher power consumption. For example, in [25] the authors have designed acoustic transceivers for communicating distances over 30–60 m with a power consumption of 8 W. Similar power consumption is also reported for longer range acoustic communication in [26]. Also the propagation of acoustic waves is slow (roughly 1500 m/s in water) as compared to electromagnetic waves, and the available communication bandwidth is quite limited due to the difficulty of making high frequency acoustic signals [27]. MI communication is also shown to provide higher data rate through materials than acoustic techniques [28]. The attenuation constant of acoustic signals also vary a lot depending on the types of tissues or bones the signal is passing [29]. The MI channels also suffer from smaller signal fluctuations and multi-path effects.

Although MI communication has been studied for some RF-challenged environments such as underwater [30], underground [31], and Body Area Networks [23], its practical use in the very dense $F^2\pi$ context poses several new challenges that we address in this paper. A key challenge is to localize the shipping boxes so that the quality of the corresponding food packages can be tracked in real time while on transit. We exploit *the regular geometry of the shipping boxes and the information of their neighbor relationship* to develop a novel Magnetic induction based Localization scheme, named MagLoc. To the best of our knowledge, this is the first proposal that explores the MI-based techniques for designing communication and localization mechanisms in this very challenging operating environment of food quality monitoring systems.

3.2. NFMI communication overview

As stated earlier, NFMI works by the principle of resonant inductive coupling between two coils. Consider a transmit and receive coil pair separated by distance r with the plane of the coils tilted at angles β_t and β_r relative to the axis joining the coil centers, as shown in Fig. 4(a). Then the magnetic field induced in a receiver coil due to the current flowing through the transmit coil is given by Lenz's law; the mutual inductance in between the coils can described as [32–34].

$$M_{t\to r} = M_{r\to t} \approx \frac{\mu\pi\mathbb{N}_t\mathbb{N}_r\rho_t^2\rho_r^2}{2r^3}\left|\cos\beta_t\cos\beta_r - \frac{1}{2}\sin\beta_t\sin\beta_r\right| \tag{1}$$

Here ρ_x and $\mathbb{N}_x$ are the radius and the number of turns in the transmit ($x = t$) and receive ($x = r$) coils respectively, and μ is the magnetic permeability of the medium. In this paper, we assume that the transceivers are of identical dimensions, i.e. $\mathbb{N}_t = \mathbb{N}_r = \mathbb{N}$ and $\rho_t = \rho_r = \rho$.

It can be seen that the induced magnetic field (and hence the induced current) in the receive coil is maximum when the planes of the two coils are aligned (i.e., $\beta_t = \beta_r = 0$), and goes down rapidly as the mis-orientation increases. In our application, it is important that the induction be roughly isotropic so that the S&C modules can be "thrown" into boxes in any orientation. This requires a "ball" like structure with 3 orthogonal coils as shown in Fig. 4(b). Because of the orthogonality, the overall field is simply a superposition of 3 fields. We have developed detailed equations for this case in [4]; here we only briefly illustrate some numerical results.

Fig. 5 shows the comparison of unidirectional and tri-directional coil transceivers with different coil orientations. μ and $\mathbb{N}$ are assumed to be $4\pi \times 10^{-7}$ Henrys/m and 10 respectively. We keep $r = 1$ m and the source voltage of the transmit coil $V_s = 3$ V in Fig. 5. The load resistance of the coils is assumed to be of 1 Ω. In Fig. 5, we keep the coil position fixed, whereas the coil orientations

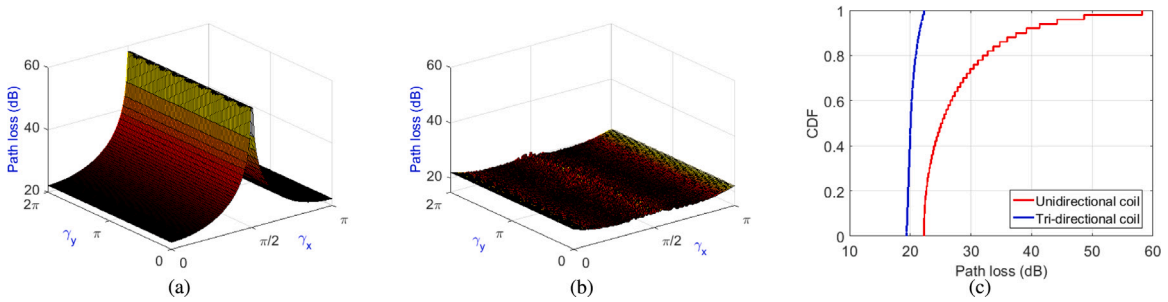

Fig. 5. Path loss in case of (a) unidirectional and (b) tri-directional coil transceivers. (c) CDF of path loss for unidirectional coil and tri-directional coil transceivers. γ_x and γ_y denote the relative angle of the coils with respect to the x and y-axis respectively.

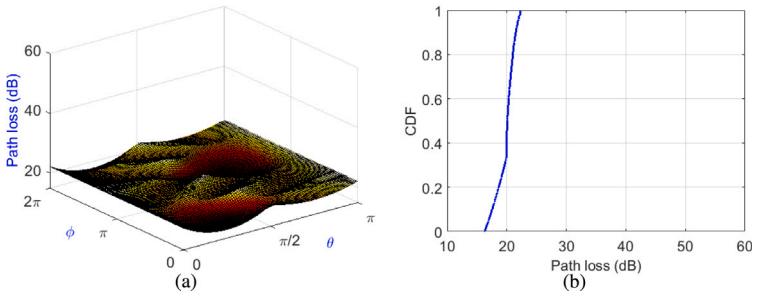

Fig. 6. (a) Path loss and its (b) CDF for tri-directional coil transceivers with different ϕ and θ. ϕ and θ are the inclination and azimuth angle of the spherical coordinate system respectively.

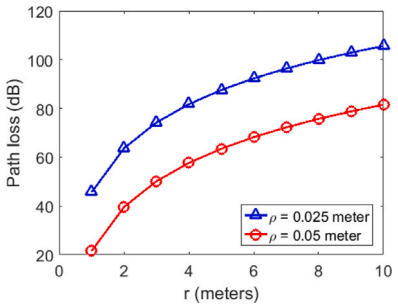

Fig. 7. Path loss with distance for tri-directional coil transceivers.

are varied with respect to its x and y axis. Notice that for the tri-directional coil, the orientation (γ_x and γ_y) in Fig. 5(a)–(b) denotes the orientation of one of the three unidirectional coils. The other two coil's orientation vary with respect to the first one, such that all three coils are orthogonal. From this figure we can observe that tri-directional coil transceivers exhibits near-isotropic transmission characteristics, which makes it suitable for our application. Also the tri-directional coil has lower path loss compared to the unidirectional coil as seen from Fig. 5(c).

We next keep the receiver coil orientation fixed, and change its relative position in the 3D space by varying the ϕ and θ, where ϕ and θ are the inclination and azimuth angle as shown in Fig. 4(c). The result is shown in Fig. 6, where r is assumed to be of 1 m. Fig. 6 demonstrates that as far as the distance in between the coils are the same, their relative positions in the 3D space do not affect the received signal strength in between them.

Fig. 7 shows the path loss with different transceiver distances using tri-directional coil transceivers. From this figure we can observe that with V_s = 3 V, the transmission range of tri-directional coil transceivers are ~2–3 m (considering 70 dB of loss) with ρ = 0.025 m and even higher with larger coil radius, which is adequate for our applications.

In practice a network will consists of multiple nodes, therefore, there will be multiple such tri-directional coils with interdependent mutual inductances in between them. The mutual inductances between any two coils can be calculated using Eq. (1), which can be utilized to calculate the induced current and received power. Using this the power received at each node is calculated by adding the received power in its three coils.

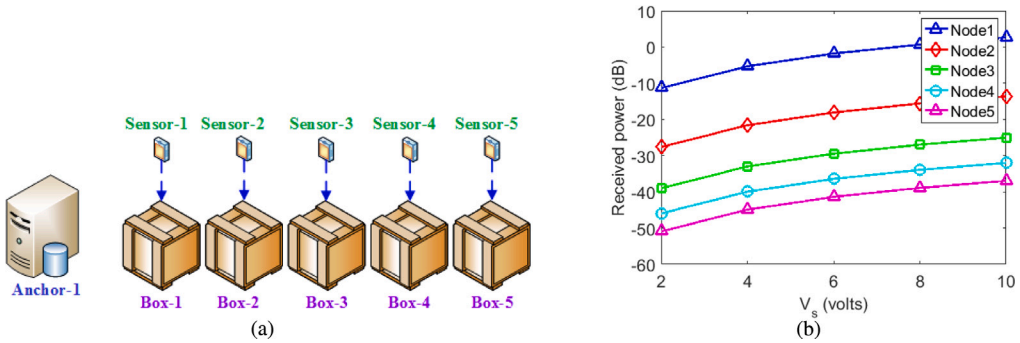

Fig. 8. (a) An illustrative example of the placement of the boxes and the sensor nodes. (b) Received power at the sensor nodes with different source voltages.

4. MagLoc : A MI based localization scheme

In this section we describe our MI based localization scheme MagLoc, its challenges and why the problem is unique as opposed to other localization problems. We assume that at the time of localization the overall box placement architecture (i.e. the boxes are kept in $10 \times 5 \times 5$ grid architecture) is known to the central controller; this assumption is practically feasible in future smart food logistics where the loading–unloading of the shipping boxes will be largely done in an automated fashion for well-planned, efficient truck space utilization. However in a large food distribution chain it is difficult to keep track of exact box (or sensor) locations. To cope up with this, we formulate the problem as follows. We assign *virtual box (VB)-ids* to the boxes enumerating their locations; for example, VB-ids can be based on their center coordinates in x, y, z axis w.r.t a reference point (i.e. in Fig. 2(b) the reference point can be one of the bottom left corners of the truck where the boxes are kept). Thus, if we can assign the sensors to the VB-ids, then we can localize the sensors (or the boxes) from their corresponding VB-id coordinates, w.r.t some reference point. Thus the purpose of MagLoc is to identify from where (i.e. from which virtual box location) the sensed data is coming, or to identify the relative positions of the shipping boxes having products that may have contamination or spoilage. In the following, we use the term *virtual box* to denote that their locations are known (w.r.t some reference point).

4.1. A conceptual overview

Ideally for localizing the sensor nodes we need to estimate their distances from some reference points (or anchors), however such techniques are not adequate in our application due to the following reasons:

1. In presence of multiple such MI coils, their interdependent mutual inductance make the distance estimate highly erroneous.
2. Finding the distance estimate requires precise knowledge of the channel parameters which is difficult to obtain in our applications, as they vary depending on the types of the food products or whether the truck (or boxes) are fully loaded or not etc.
3. The distance estimate also requires the exact coil orientations, which is also not available in this scenario as different boxes can be kept in different orientations during loading–unloading.
4. The magnetic signals in such environments are also influenced by the ferromagnetic walls (of the trucks, carriers etc.), which makes the problem even more challenging.

Therefore in contrast to such distance based localization schemes [34,35], our objective is to collect the information of the received power at the sensor nodes from an anchor to get their relative distance order with respect to that anchor and use this information to localize them to the known virtual box positions. We argue in Section 4.4 that such an approach is robust even in presence of the truck walls.

We first explain the concept of MagLoc using Fig. 8(a) where 5 cubic boxes with dimensions (Δ) equal to 1 m are deployed side by side. We assume that a sensor node is placed at the center of each box. There is one anchor node that transmits pilot signals; the received power from these pilot signals are recorded by the 5 sensor nodes. Let us assume that B_i and S_i denote box-i and sensor-i respectively; box B_1 is closest to the anchor whereas B_5 is the farthest.

Fig. 8(b) shows that variation of the received powers at the sensor nodes with different voltage V_s. From Fig. 8(b) we can observe the following characteristics. First, the receiver power at the sensor nodes increases with the increase in V_s. Second, the received powers are consistent with the box distances from the anchor, i.e. the received power of S_1 is the highest whereas that of S_5 is the lowest; in fact, this trend remains consistent with different V_s. Thus, if we maintain any constant V_s at an anchor, then we can obtain relative order of the sensor node's positions from that anchor; which can be matched with that of the virtual boxes to get an indication of which sensor nodes is kept in which virtual box. However, this order can be disturbed in presence of higher number of sensor nodes, due to the mutual inductance in between their coils. Furthermore, the relative order may also be disturbed as the propagation characteristics of the tri-directional coils are not completely isotropic, as observed in Fig. 5(b).

In order to study the impact of many sensors, we develop a factor called *outlier factor* which is defined as follows. Consider a scenario where N boxes (along with sensing devices) are placed in a 3-D grid such that the ith sensor node is placed in the ith box.

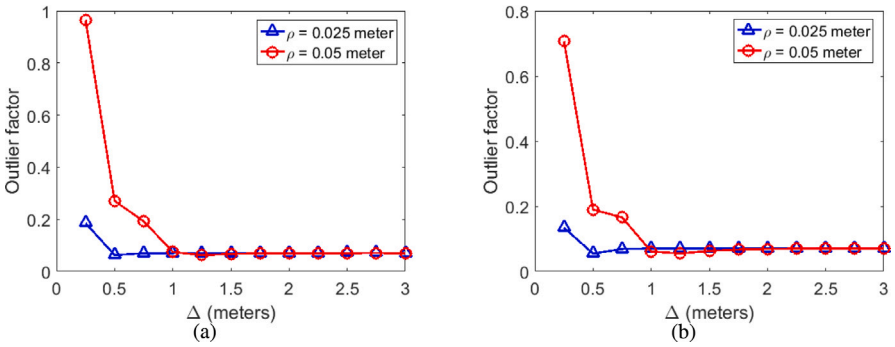

Fig. 9. Variation of outlier factor with different Δ, in case of (a) 125 sensor nodes, and (b) 250 sensor nodes.

An anchor is placed at one corner of the grid with enough power to reach all nodes. We assume that $\mathbb{S}_{ig}$ is a matrix which is 1 if the received power of sensor node S_i is more than that of S_g, and $\mathbb{B}_{ig}$ is 1 if box B_i is closer to the anchor than box B_g. With this we define the outlier factor as $\frac{\sum_i \sum_g |\mathbb{S}_{ig} - \mathbb{B}_{ig}|}{\sum_i \sum_g \mathbb{S}_{ig}}$, i.e. the outlier factor measures the level of inconsistencies between the power received by the sensor nodes and their corresponding box distances from the anchor. For example in Fig. 8(b) the outlier factor is 0, as the received power is consistent with the box distances from the anchor.

Fig. 9 shows the variation of the outlier factor with different Δ. We consider two cases: Fig. 9(a) shows the outlier factor with a 3-D grid of $5 \times 5 \times 5$ boxes, whereas Fig. 9(b) shows the scenario with $10 \times 5 \times 5$ boxes. From Fig. 9 we can observe that even with $\rho = 0.05$ m and $\Delta = 0.5$ m, the outlier factor remains below 0.4 both in case of 125 and 250 sensor nodes, i.e. less than 40% of the relative ordering are inconsistent whereas the rest are consistent. However the outlier factor is significantly low (below 0.2) when the coil radius $\rho = 0.025$ m. This is because higher coil radius leads to larger effect of mutual inductance in between the coils, which results in higher outlier factor. Therefore, from this point onwards we keep the coil radius $\rho = 0.025$ m because of its smaller outlier factor and thus for better localization accuracy. The transmission range with $\rho = 0.025$ m is 2–3 m which is adequate for our purpose. In addition to that keeping the coil size small makes it easier to attach it in small food boxes.

4.2. Localization problem formulation

We assume that there are N sensor nodes that are placed in N shipping boxes. Also assume that A anchors are placed at different corners at the trucks (or warehouses) whose transmissions can be received by all the sensor nodes; this assumption can be feasible in many scenarios as the anchors are not battery constrained and thus use higher V_s to extend their transmission ranges. Later on in Section 5.2.3 we will show that this assumption can be relaxed. While localizing the boxes, the anchor nodes broadcast *pilot* signals, which carry the ids of the corresponding anchors; we assume that the pilot signals from different anchors are transmitted at different time scales so that they do not interfere, which can be achieved by coordination among the anchors. Upon receiving these pilot signals, the sensor nodes record the received power corresponding to these signals from different anchors and report them to the sinks (which then report them to the central controller through WiFi interface) using multi-hop communications.

The central controller then exploits (a) the known virtual box locations and their relative distance order from each anchor, and (b) the relative distance order of the sensor nodes from each anchor based on their received power from the anchors, to assign the sensor nodes to the virtual boxes. The overall localization problem formulation at the central controller can be described as follows. Assume that x_{ig} is a binary decision variable which is 1 if the sensor node S_i is assigned to virtual box B_g. Also assume that d_i^a denotes the distance between anchor-a and the box B_i. $\mathbb{S}_{if}^a$ is an input binary variable which is 1 if $\mathcal{P}r_i^a > \mathcal{P}r_f^a$, and $\mathbb{B}_{gl}^a$ is also an input binary variable if virtual box B_g is closer to a than box B_l, i.e. $d_g^a < d_l^a$. With these the problem of MagLoc can be formulated as follows:

$$\text{Maximize} \sum_{a=1}^{A} \sum_{i=1}^{N} \sum_{g=1}^{N} \sum_{f=1}^{N} \sum_{l=1}^{N} x_{ig} x_{fl} \mathbb{S}_{if}^a \mathbb{B}_{gl}^a \tag{2}$$

where $x_{ig} \in \{0, 1\} \quad \forall i \in \mathcal{S}, g \in \mathcal{B}$ and

$$\sum_{g=1}^{N} x_{ig} = 1, \ \forall i \in \mathcal{S}, \qquad \sum_{i=1}^{N} x_{ig} = 1, \ \forall g \in \mathcal{B} \tag{3}$$

where $\mathcal{S}$ and $\mathcal{B}$ are the set of sensor nodes and boxes. The objective is to assign the sensor nodes into the virtual boxes such that the similarities in between the distance order of the sensor nodes and the virtual boxes are maximized. For example assume that the sensor node S_i is assigned to virtual box B_g, and the sensor node S_f is assigned to virtual box B_l. In such a scenario, if $\mathcal{P}r_i^a > \mathcal{P}r_f^a$ and $d_g^a > d_l^a$, then $\mathbb{S}_{if}^a = 1$ and $\mathbb{B}_{gl}^a = 0$. Thus the expression $x_{ig} x_{fl} \mathbb{S}_{if}^a \mathbb{B}_{gl}^a$ becomes 0, or there is a discrepancy in the distance orders corresponding to this assignment. On the other hand if $d_g^a < d_l^a$, then $x_{ig} x_{fl} \mathbb{S}_{if}^a \mathbb{B}_{gl}^a$ equals to 1, which says that the assignment conforms the corresponding distance orders. Constraints (3) ensure that a sensor node is assigned to exactly one virtual box and vice versa.

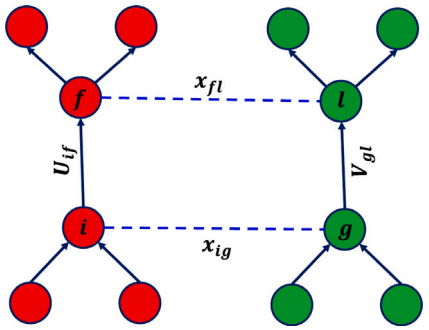

Fig. 10. Rectangle rule for subgraph isomorphism with red & green nodes for graphs **U** and **V**.

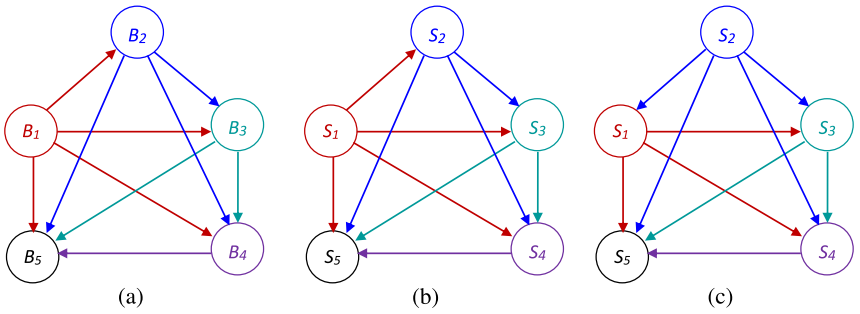

Fig. 11. Constructing the directed graphs of (a) $\mathbb{B}^1$ and (b) $\mathbb{S}^1$ corresponding to Fig. 8, whereas (c) represents a scenario where $\mathcal{P}r_2^1 > \mathcal{P}r_1^1$. B_i and S_i denote virtual box-i and sensor node-i respectively.

Theorem 1. *The problem of magnetic localization is NP-hard.*

Proof. We first define the *largest common subgraph* problem (LCS) which is known to be NP-complete. Graph H is said to be *common* to graphs G_1 and G_2 if both G_1 and G_2 contain induced subgraphs isomorphic to H. The maximum common subgraph problem can be defined as follows: given a pair of graphs G_1 and G_2, find the largest induced subgraph common to both.

We now show that our magnetic localization problem contains the largest common subgraph problem as a special case. Assume an instance of the magnetic localization problem with $A = 1$, then $\mathbb{S}^1$ and $\mathbb{B}^1$ are two $N \times N$ adjacency metrices. We construct two directed graphs **U** and **V** such that $U_{ig} = \mathbb{S}^1_{ig}$ and $V_{ig} = \mathbb{B}^1_{ig}$. Then a graph H is the largest common subgraph of **U** and **V** if and only if the maximum value of Eq. (2) is equal to the number of edges in H. This can be verified by using the rectangle rule of subgraph isomorphism as mentioned in [36], i.e. when $x_{ig} = x_{fl} = U_{if} = V_{gl} = 1$ in (2) it forms a rectangle as shown in Fig. 10. Thus finding the maximum of (2) is equivalent to finding the number of such rectangles. This is equivalent to finding the maximum number of common links of **U** and **V**, or in turn solving the largest common subgraph problem. Since the largest common subgraph problem is NP-complete and a special case of the magnetic localization problem, thus our magnetic localization problem is NP-hard. □

4.3. Proposed heuristic

As the problem is NP-hard we propose a heuristic solution for assigning the sensor nodes to the boxes, which is discussed in Algorithm 1. The idea is to consider $\mathbb{B}^a$ and $\mathbb{S}^a$ as two directed graphs, and then to best match the vertices of these two graphs. For example, Fig. 11 shows the example of $\mathbb{B}^1$ and $\mathbb{S}^1$ corresponding to the box and sensor placement of Fig. 8. In Fig. 11(a) there is a directed edge from B_i to B_j if $d_i^1 < d_j^1$, whereas a directed edge between sensors S_i to S_j in Fig. 11(b) represents $\mathcal{P}r_i^1 > \mathcal{P}r_j^1$. Thus by computing the graph matching in between $\mathbb{B}^1$ and $\mathbb{S}^1$ we can find out that sensor nodes $(S_1, S_2, S_3, S_4, S_5)$ are placed in virtual boxes $(B_1, B_2, B_3, B_4, B_5)$. On the other hand Fig. 11(c) represents the scenario where $\mathcal{P}r_2^1 > \mathcal{P}r_1^1$, thus there is a directed edge between sensor S_2 to S_1. Solving the graph matching in between Fig. 11(a) and (c) reveals that $(S_1, S_2, S_3, S_4, S_5)$ are placed in $(B_2, B_1, B_3, B_4, B_5)$.

We thus propose a graph matching scheme to find out which sensor nodes are placed in which boxes, by developing a heuristic which is inspired by [36]. We first modify the objective function of Eq. (2)

$$E = \sum_{a=1}^{A} \sum_{i=1}^{N} \sum_{g=1}^{N} \sum_{f=1}^{N} \sum_{l=1}^{N} x_{ig} x_{fl} \mathbb{S}^a_{if} \mathbb{B}^a_{gl} \tag{4}$$

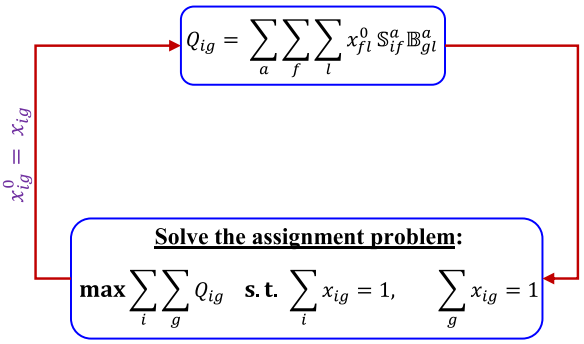

Fig. 12. The iterative procedure for assigning sensor nodes to boxes.

using Taylor series expansion as follows:

$$E \approx \sum_{a=1}^{A} \sum_{i=1}^{N} \sum_{g=1}^{N} \sum_{f=1}^{N} \sum_{l=1}^{N} x^0_{ig} x^0_{fl} \mathbb{S}^a_{if} \mathbb{B}^a_{gl} + \sum_{i=1}^{N} \sum_{g=1}^{N} Q_{ig} \left(x_{ig} - x^0_{ig} \right)$$

$$\text{where } Q_{ig} = \frac{\partial E}{\partial x_{ig}} \Big|_{x_{ig}=x^0_{ig}} = \sum_{a=1}^{A} \sum_{f=1}^{N} \sum_{l=1}^{N} x^0_{fl} \mathbb{S}^a_{if} \mathbb{B}^a_{gl} \tag{5}$$

In Eq. (5) x^0_{ig} is assumed to be the initial estimate of x_{ig}. Thus maximizing the above Taylor expansion is equivalent to

$$\text{Max} \sum_{i=1}^{N} \sum_{g=1}^{N} Q_{ig} x_{ig} \quad \equiv \quad \text{Min} \sum_{i=1}^{N} \sum_{g=1}^{N} C_{ig} x_{ig} \tag{6}$$

$$\text{s.t.} \sum_{g=1}^{N} x_{ig} = 1, \ \sum_{i=1}^{N} x_{ig} = 1, \ x_{ig} \in \{0, 1\} \tag{7}$$

where $C_{ig} = \mathbb{M} - Q_{ig}$ for any large number $\mathbb{M}$. The purpose of replacing Q_{ig} by C_{ig} is to convert the above problem as an *assignment problem* which can be solved by using the *Hungarian assignment* scheme [37] in polynomial time.

We thus propose an iterative procedure as follows. We first start with an initial value of x_{ig} and expand the first order Taylor series by taking the partial derivative to calculate Q_{ig} using Eq. (5). We next use the Hungarian scheme corresponding to that Q_{ig} to get an initial assignment by solving the assignment problem of Eqs. (6)–(7). This outcome of the assignment problem or x_{ig} is next used to calculate the modified Q_{ig} from Eq. (5). This process is repeated until the solution converges or a maximum number of iterations $I_{\max}$ is reached. The iterative procedure is pictorially depicted in Fig. 12.

Algorithm 1 Proposed heuristic solution of MagLoc for assigning the sensor nodes to individual virtual boxes

A: Number of anchors ▷ INPUT
$\mathbb{S}^a$: Order matrix of the sensor nodes corresponding to anchor-a ▷ INPUT
$\mathbb{B}^a$: Order matrix of the virtual boxes corresponding to anchor-a ▷ INPUT
x_{ig}: Whether or not the sensor node-i is in virtual box-g ▷ OUTPUT

procedure MagLoc
x^0 is initialized to any random assignment matrix;
  while x is not converged or number of iterations $< I_{\max}$ **do**
    $Q_{ig} = \sum_{a=1}^{A} \sum_{f=1}^{N} \sum_{l=1}^{N} x^0_{fl} \mathbb{S}^a_{if} \mathbb{B}^a_{gl} \ \forall \ i, g$;
    Use Hungarian method to get an assignment x_{ig};
    $x^0_{ig} = x_{ig}, \ \forall \ i, \ g$;
  end while
Return the assignment $x_{ig}, \ \forall \ i, \ g$;
end procedure

4.4. Effects of the truck walls

In a food transportation scenario, the localization of boxes carried on a carrier (e.g., truck) may be disturbed by the ferromagnetic (mild steel) materials inside of the truck walls, since the anchors will be mounted on those walls. Using the so called *image theory* [38], we show that the presence of a ferromagnetic wall will not have any detrimental effect on the localization accuracy. We illustrate this using Fig. 13(a) where a coil carrying current I is placed at a distance z_0 from the truck wall of thickness w. According to the image theory, this will result in a *primary* image at $-z_0$ (with current αI), and multiple *secondary* images at $z = -(2nw + z_0)$

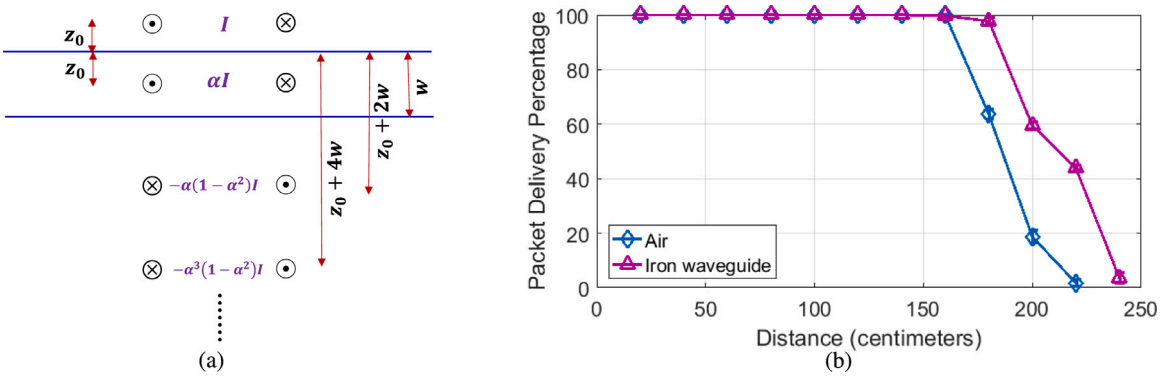

Fig. 13. (a) Illustration of image theory where the width of the ferromagnetic walls is w. (b) Effect of iron waveguide on transmission range.

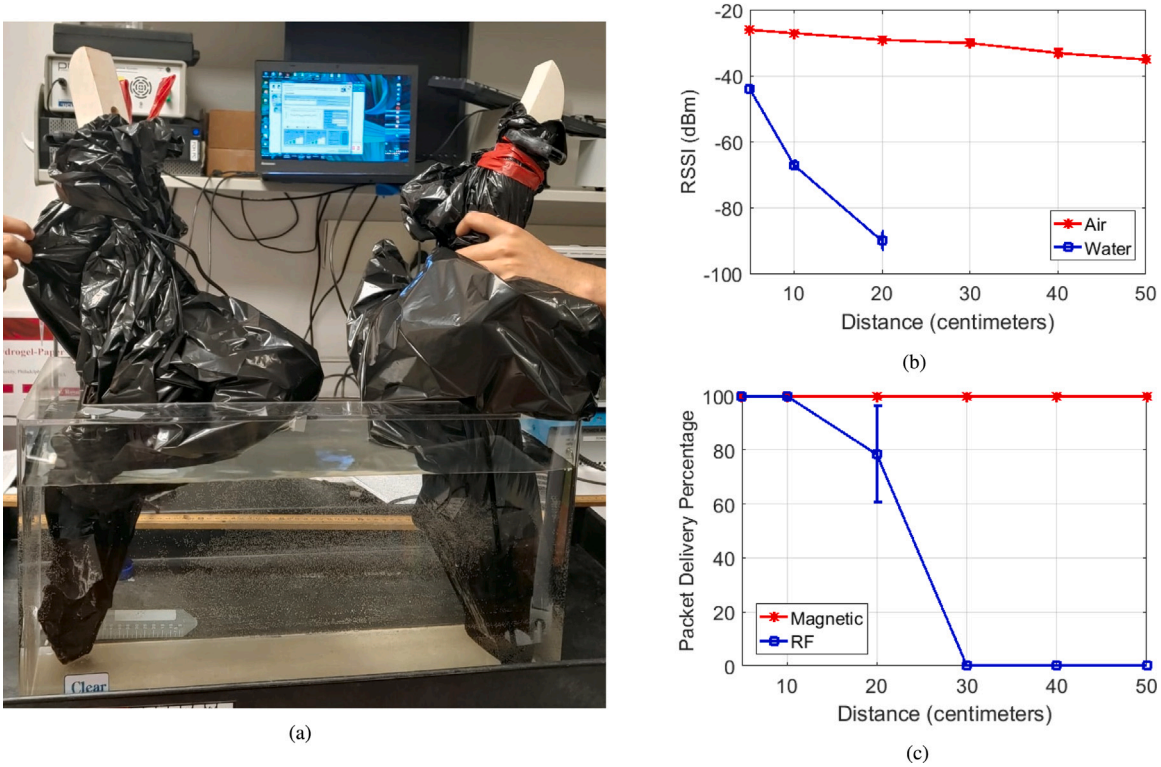

Fig. 14. (a) Underwater environment for the comparison of propagation characteristics between RF and magnetic communications. (b) Comparison of RF RSSI in air and water media. (c) Comparison of packet delivery percentage for RF and magnetic communication in underwater environment.

(with current $\alpha^{2n-3}(1-\alpha^2)I$), for $n \geq 2$. Here $\alpha = \frac{\mu_r - 1}{\mu_r + 1}$, where μ_r is the relative permeability of the truck material. For ferromagnetic materials with high μ_r, $\alpha \approx 1$, i.e. the secondary images become insignificant, whereas the primary image will only enhance the magnetic signal. Thus, the relative ordering of sensors (derived from signal strength) will remain unchanged even in presence of ferromagnetic walls.

To experimentally demonstrate the effect of image theory, we build a small prototype using the FlexMI/Freelinc boards plus EMBware development boards [39]. The Freelinc Near Field Magnetic Induction based radios [40] have transmitters that are equipped with 3-axis magnetic coils to provide near-isotropic communication characteristics. We place an iron plate behind the transmitter to imitate the scenario of Fig. 13(a). Fig. 13(b) compares the transmission range of MI packet delivery ratio of MI communication in air medium along with and without the presence of an iron waveguide. We have observed that using the iron plate as an waveguide indeed enhances the transmission range by few centimeters. This is because an iron plate essentially acts like a mirror which "reflects" the magnetic flux and strengthen the signal.

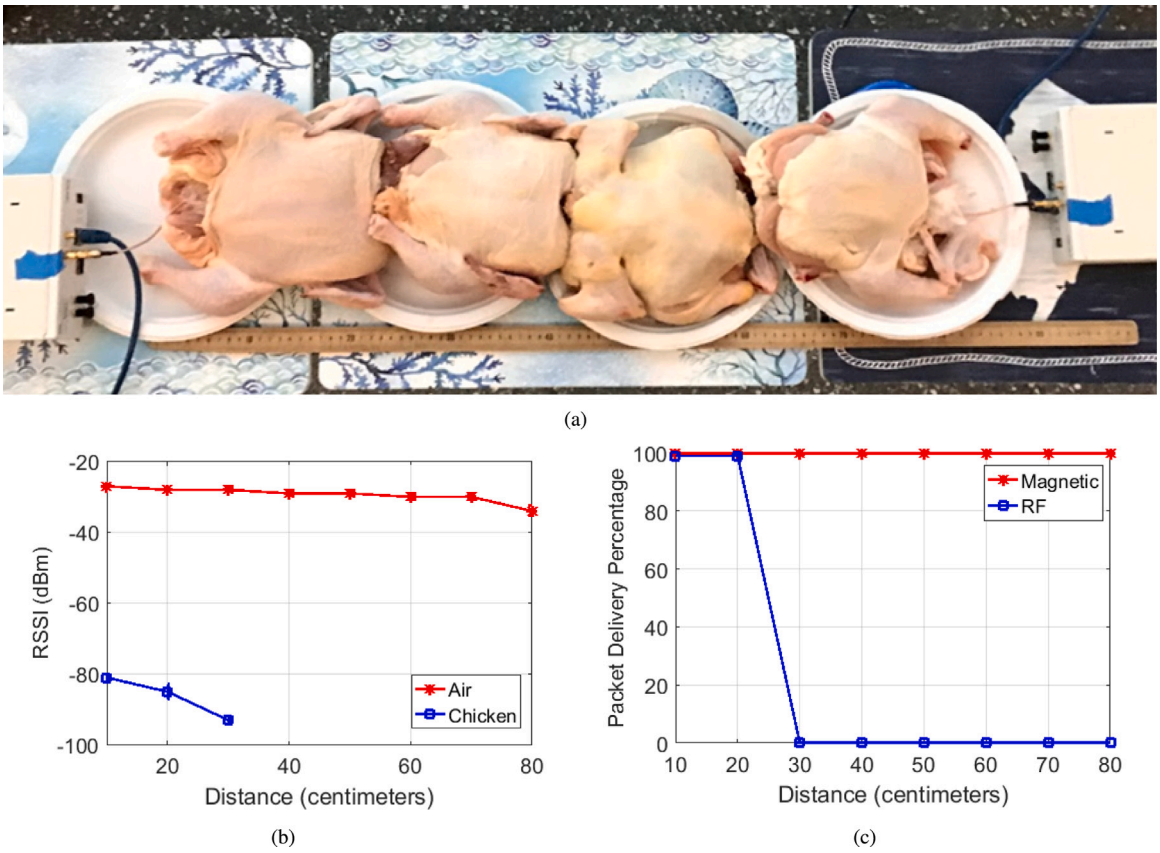

Fig. 15. (a) Experimental setup for the comparison of propagation characteristics between RF and magnetic communications. (b) Comparison of RF RSSI in air and chicken media. (c) Comparison of packet delivery percentage for RF and magnetic communication inside chicken medium.

The robustness of MagLoc even in presence of ferromagnetic objects makes this particularly suitable for our application,[1] rather than other distance based localization schemes studied in [34,35]. On the other hand for the trucks with wooden walls, the relative permeability of the truck walls is so low that their effects become insignificant.

5. Performance evaluation

Ideally, the evaluation of the scheme should be done with a real food distribution environment with multiple food boxes stacked inside a truck or in a warehouse, however, this is simply not possible in practice. As a result, we have done an experimental comparison between RF and MI communication inside a lab environment to show the superiority of MI communication over RF in aqueous and tissue medium in Section 5.1. Other than that the evaluation of MagLoc is largely based on simulations that account for the MI communication characteristics in Section 5.2.

5.1. Experimental comparison between RF and MI

The primary factor affecting the propagation of electromagnetic waves through fresh food is the water and mineral content. For example, strawberries, watermelon, spinach, broccolis contain ~91%–92% of water, whereas apples, pears, pineapples contain ~84%–87% of water [41]. Similarly different meat products contain ~56%–71% water [42]. For the experiments we first used a water filled glass tank of dimension $50 \times 30 \times 20$ cm^3, as shown in Fig. 14(a). We use the XBee module (www.digi.com/xbee) as the RF transceivers, whereas the Freelinc boards are used a MI radios, both with a transmit power of 0 dBm.

We first compare the RF path loss in air and aqueous medium in Fig. 14(b). It is seen that received signal strength decay with distance is rather slow in the air (−38 dBm at 50 cm), but very steep for water (−90 dBm at only 20 cm). This shows the key limitation of RF communication in aqueous medium, which makes it unsuitable for use inside the food boxes. Fig. 14(c) shows the

[1] MagLoc is also useful when all the nodes have identical orientations, which is possible for a futuristic, completely automated packing and loading–unloading environment. In fact in case of identical node orientations, a single coil (instead of 3-coils) can also be used for successful communication and localization.

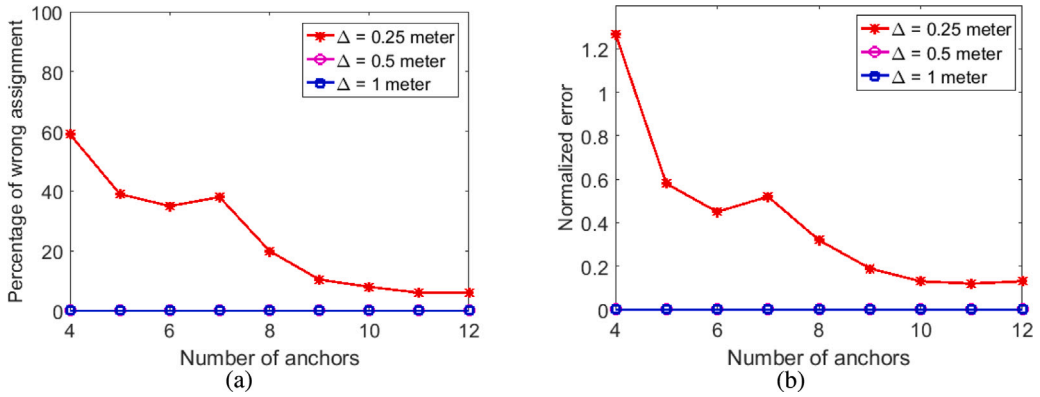

Fig. 16. (a) Percentage of wrong assignment when 125 boxes are kept in a 5 × 5 × 5 grid. (b) Average normalized error.

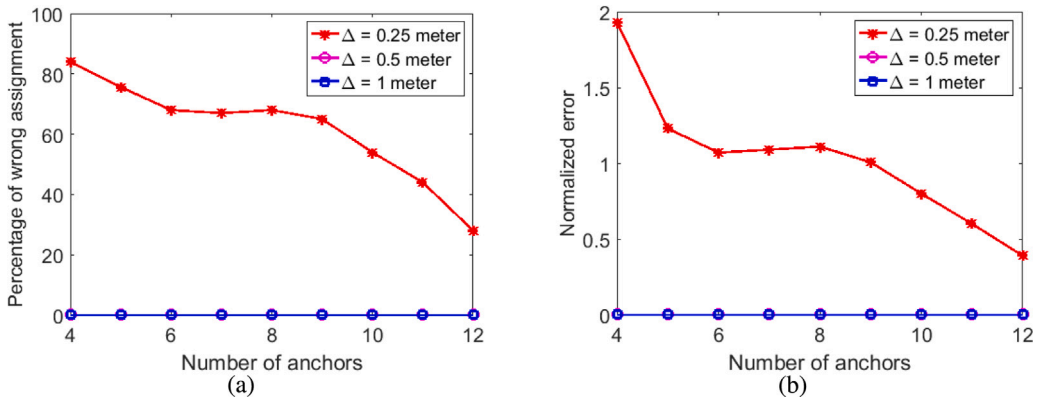

Fig. 17. (a) Percentage of wrong assignment when 250 boxes are kept in a 10 × 5 × 5 grid. (b) Average normalized error.

comparison of packet delivery ratio of RF and MI communication in the aqueous medium. Notice that we did not plot the RSSI measurements for MI communication in Fig. 14; this is because the Freelinc radios do not provide RSSI values. From this figure we can observe that MI communication from the Freelinc transceivers can easily communicate up to a distance of 50 cm, whereas the RF communication range is limited to about 20 cm. This clearly shows the superiority of MI communication in aqueous medium as opposed to RF.

To demonstrate the effect of food medium on RF communication, we have conducted an experiment on whole chicken and inserted the radios inside the chicken as shown in Fig. 15. Fig. 15(b) shows the received signal strength at the receiver with RF radios in air and inside chicken medium. The signal strength drops to −93 dBm at 30 cm, and so no successful RF transmission can take place beyond 20 cm. However, the Freelinc radios can easily penetrate through the tissue medium and thus can communicate successfully within 1 m of transceiver separation as observed in Fig. 15(c).

5.2. Simulation results

We next evaluate the accuracy of the MagLoc scheme using Matlab simulations. We assume that some food boxes are kept in a grid fashion, which is similar to that of Fig. 2(b). We vary the number of boxes to create two different scenarios: (a) in the first scenario 125 boxes are placed in a 5 × 5 × 5 grid, whereas (b) in the second scenario we consider 250 boxes placed in a 10 × 5 × 5 grid. We assume that these boxes are cubic and symmetric with dimension Δ, however the proposed scheme can also be applied with different box dimensions. In our simulation, we consider the worst case scenario where the minimum Δ is assumed to be 0.25 m, however, in reality typical food boxes are even more than 0.5–1 m. We record two performance indicators to evaluate the accuracy of MagLoc: (a) the first one is the percentage of the sensor nodes that are assigned to wrong virtual boxes, whereas (b) the second one if the normalized error which is equal to $\left(\frac{\text{distance error between actual and prescribed box centers}}{\Delta}\right)$. Basically the normalized error gives an estimation that if a spoiled package is not found in its prescribed box, then how many neighboring boxes need to be searched to find that package.

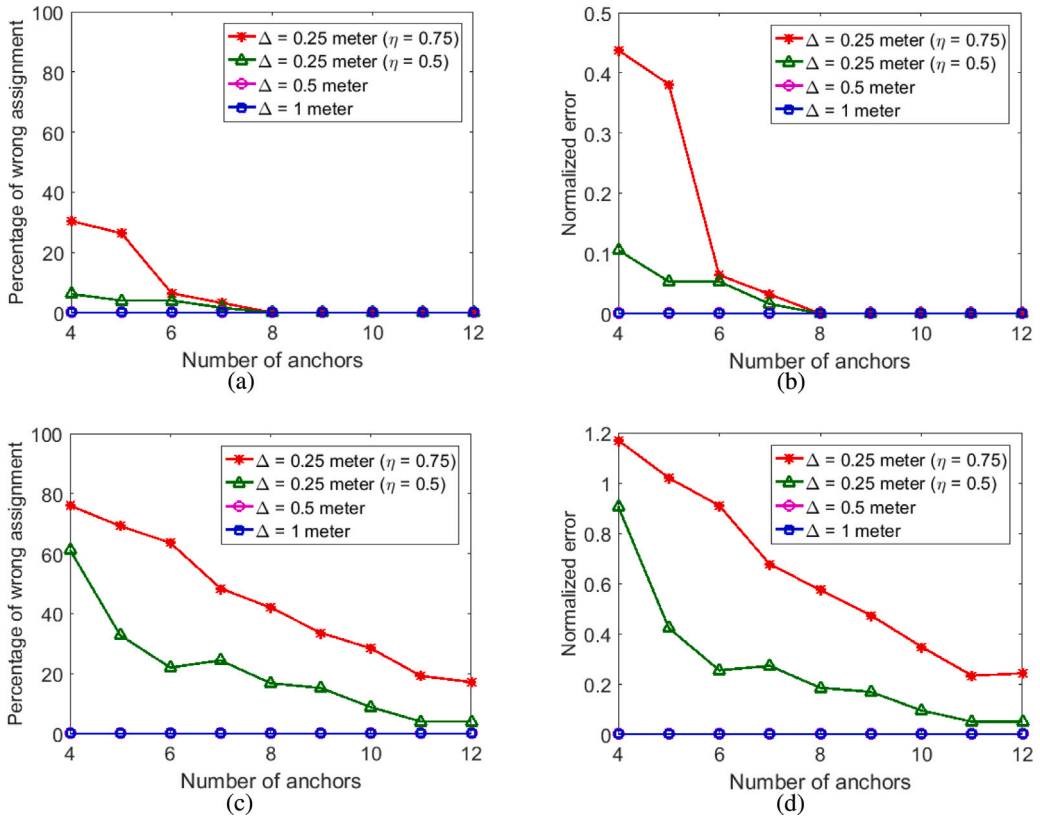

Fig. 18. (a)–(c) Percentage of wrong assignment with 125 and 250 boxes respectively, along with their (b)–(c) average normalized errors.

5.2.1. Results for 125 boxes

Fig. 16(a)–(b) show the performance of MagLoc in case of 125 boxes. From Fig. 16(a) we can observe that the percentage of wrong assignment is zero as far as Δ is more than or equal to 0.5 m. With $\Delta = 0.25$ m we can observe some wrong assignments, which reduces by ∼55% as the number of anchors increase from 4 to 12. Fig. 16(b) demonstrates that the average normalized error with different number of anchors and Δ. While comparing Fig. 16(a)–(b) we can observe that when the number of anchors is less than 5 and $\Delta = 0.25$ m, the percentage of wrong assignment is above 40%. However even in such cases the average normalized error is less than 2, i.e. the targeted box can be found within 2 boxes in the neighborhood of the prescribed box. Fig. 16(b) also demonstrates that the average normalized error reduces by ∼85% when the number of anchors is increased from 4 to 12.

5.2.2. Results for 250 boxes

Fig. 17(a)–(b) demonstrates the performance of MagLoc with 250 boxes. From Fig. 17 we can observe that with $\Delta = 0.25$ m, the percentage of wrong assignment is significantly high when the number of anchors is low. However the average normalized error is still less than 2 in all cases. The amount of wrong assignment is reduced significantly (∼50%) when the number of anchors is increased from 4 to 12. We have also observed that with 12 anchors and $\Delta = 0.25$ m (not shown in the figures), for more than 90% of the sensor nodes the normalized error is less than 1, even the maximum error is less than 2.

From these evaluations we can conclude that using MagLoc the percentage of miss-assignment is significantly low and goes to zero as long as the Δ is more than or equal to 0.5 m. In a real food logistics, typically the large boxes carrying multiple small food packages are indeed more than 0.5–1 m. In these scenarios, our MagLoc scheme can effectively localize the nearly spoiled or contaminated boxes with sufficiently high level of accuracy so that they can be easily isolated.

5.2.3. Effects of partial transmission coverage of the anchor nodes

For Figs. 16–17 we assume that the pilot signal emitted by the anchors nodes can be received by all the sensor nodes. We now show the effects of limited transmission coverage of the anchor nodes in Fig. 18. We assume that the anchors have a transmission coverage of $\eta\Delta\ell$ where ℓ is the maximum number of boxes along any grid axis, and $0 \leq \eta \leq 1$. The transmission coverage should be sufficient enough to ensure that all the *sensor nodes receive pilot signal from at least one anchor node*. In Fig. 18 we kept η above 0.5 to ensure this condition.

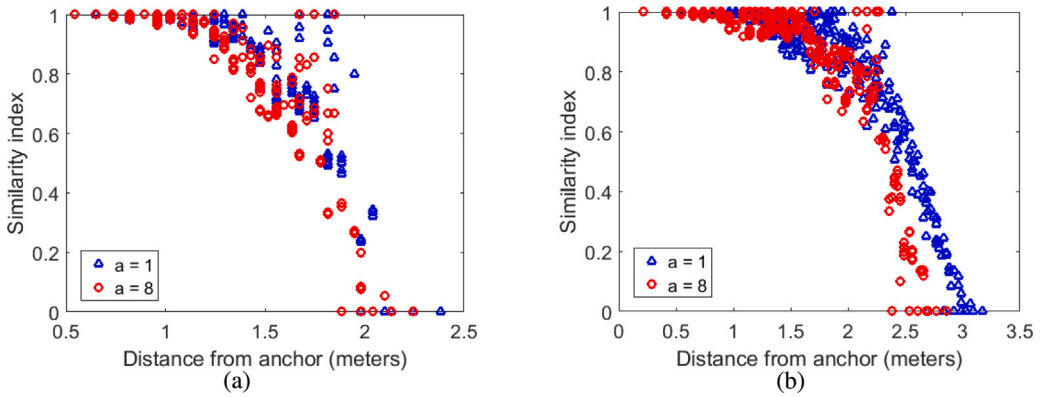

Fig. 19. Similarity index with distance from different anchors, in case of (a) 125 nodes, and (b) 250 nodes.

By comparing Figs. 16–17 and 18 we can observe that the percentage of wrong assignment and the normalized error decreases as η reduces. With 125 nodes the percentage of wrong assignment is reduced by ∼25% when η is reduced from 1 to 0.75, and even further down to ∼53% with η equal to 0.5. Similar characteristics are noticed for 250 nodes as shown in Fig. 18(c)–(d).

We explain this phenomenon with the help of Fig. 19. As the distance in between the sensor nodes decreases, the interaction in between them increase as well as the discrepancies (or the outlier factor) of their respective distance orders as observed from Fig. 9. We notice that the amount of discrepancies increase as the distance between the anchor and the sensor nodes increase. To show this effect we place 125 sensor nodes in 125 boxes such that the ith sensor node is placed in the ith box. We assume ρ and Δ to be 0.025 m and 0.25 m respectively. We then calculate the amount of similarities in between the sensor node orders and the box orders. We define a parameter named *similarity index* which is equal to $\frac{\sum_j \mathbb{S}^a_{ij} \mathbb{B}^a_{ij}}{\sum_j \mathbb{B}^a_{ij}}$ corresponding to all sensor nodes i. Fig. 19(a) shows the variation of the similarity index in between $\mathbb{S}^a$ and $\mathbb{B}^a$ with the increase in distance in between the anchor and the sensor nodes. Fig. 19(b) shows the same effect with $N = 250$ nodes. From these figures we can observe that the similarity index goes down as the distances between the anchor and the boxes increase. This significantly disturbs the accuracy of the proposed localization scheme.

From Fig. 19(a) we can observe that after 1.5 m the similarity index drops below 0.6, whereas in Fig. 19(b) the index drops below 0.6 beyond 2.5 m. Thus limiting the transmission coverage of the anchor nodes ignores the effects of mutual inductance and discrepancies caused by the sensor from the faraway boxes. This significantly improves the accuracy of the proposed localization scheme.

6. Related works

The article covers a wide range of research areas, including three primary areas of near-field magnetic communication, NFMI localization and the localization of sensor nodes, which are quite well-mined. We thus summarize the key works in these areas separately.

MI communications: Magnetic communication is proposed as an alternative to Bluetooth technology in RF challenged environments [43,44]. As the path loss of the magnetic induction based communication is very high, in [45,46] the authors have studied the effect of MI waveguide to enlarge the communication range in challenged environments. Later on magnetic induction based communication has been utilized in various environments such as for underwater communications [47,48], underground communications [46,49,50], mining disaster environments [51], underground animal tracking applications [52], pipeline monitoring applications [35,53], body area networks [54,55] etc. The communication technology is standardized by IEEE 1902.1 standard in 2009; the standard specifies a near-field communication protocol called *RuBee* which operates at a low-frequency range of 30–900 kHz [56]. The sole purpose of RuBee is to support low data rate, RF challenging applications with small battery units that can last for 5–10 years. For short range use cases, typical operating frequency of NFMI is 13.56 MHz [40]; at this frequency range, the technology achieves a data rate of 400 kbps with a range of 1–2 m. Higher range of few tens of meter is achieved at lower frequency range (i.e. 130 kHz as used in RuBee); at this range the NFMI range extends upto few tens of meter, however, the achievable rate goes down.

MI based localization: MI based localization have shown promising performance in various challenging environments, including indoor environment [57], underground environment [58,59], pipeline environment [60] etc. In these literature the authors have introduced some localization techniques for MI environments similar to the RSSI techniques with modified channel models specifically designed for MI communication. The main advantage of MI based localization as proposed in these literature is that, it is less impacted by obstacles such as walls, floors, people etc. At the same time, the communication technology is less impacted by multi-path effects as compared to RF, which improves the localization accuracy. However, MI positioning is greatly impacted in presence of ferrous materials in the vicinity of the sensing devices [61]; which makes the previous methods inapplicable and

erroneous in our food transportation environment. At the same time, these approaches use the knowledge of *precise* channel parameters to localize the sensing nodes, which is also not available in our scenario. Our work is significantly different than the previous approaches as we propose a relative order based localization technique rather than using the actual RSSI, which is inappropriate in our proposed environment. Also contrary to the other approaches, in our scheme the exact knowledge of channel parameters are not required.

Localization in sensor networks: In sensor networking context localization is well researched and a significant amount of proposals exist in the literature; in fact a number of survey articles on sensor localization can be found in [62–64]. Existing sensor localization schemes can be broadly categorized into range-based and range-free schemes [63,64]. Range based techniques include RSSI [65,66], ToA, TDoA [67,68] and AoA [69,70] techniques. In RSSI, ToA and TDoA based approaches, the signal path loss or propagation time in between the sensor nodes are translated into distance estimate, which are then used for node localization. On the other hand, AoA based approaches estimate the angle at which signals are received from different sensor nodes and use simple geometric relationships to calculate node positions. Range-free algorithms do not measure the distance or angle information between unknown nodes and anchors, rather they estimate the distance between two nodes by the connectivity information [71,72], the energy consuming information [73,74], or the area information of the superimposed region of the landmarks [75,76] etc. Our proposed localization problem itself is different than the other approaches as it requires a mapping between the sensor nodes to the shipping boxes, rather than obtaining the location estimates of the sensor nodes. The approach adopted in this paper is novel compared to the existing approaches as it uses a relative estimate of distance orders between the individual sensor nodes and the anchors, rather than using the traditional distance (or angle) estimate or connectivity information among the nodes.

7. Conclusions

In this paper, we developed an IoT based food quality sensing and communication mechanism in fresh food transportation environments using MI-based communications. By considering the unknown orientations of the sensors and complex channel models in food transportation environments, we proposed a localization scheme to localize the shipping boxes carrying perishable food packages. The major outcome of the simulation experiments is the fact that the sensor nodes are localized with acceptable accuracy as far as the box lengths have dimensions of 0.5 m or above. One of the implementation related issue of MagLoc is the deployment cost of the sensing units and radio technology. However, due to the emerging paper/plastic based sensor and flexible circuits, inkjet-printed on-chip sensors and antennas or multi-walled carbon nanotube based solutions are expected to realize such low-cost solutions where the entire sensor and radio module is inexpensive enough to be embedded in retail level packages. In fact developing paper based sensors and various forms of low-cost food sensing mechanisms are tremendously studied recently [77,78], and the proposed work on integrating the sensing and communication technology can advance this research towards a more efficient and smarter food logistics. However, it requires future research in many directions, including building inexpensive and very low-power sensing, communication and battery technologies, developing ultra-low power communication protocol for long-term operation of the sensors, exploring energy harvesting mechanism specifically for food transportation environment, along with an integrated control of sensing, localization and food-preservation methods (like temperature, humidity control) to minimize the extent of spoilage.

Declaration of competing interest

The authors declare that they have no known competing financial interests or personal relationships that could have appeared to influence the work reported in this paper.

Acknowledgments

This work was supported by NSF, USA grants under award numbers CNS-1744187 and CNS-1844944.

References

[1] B. Montreuil, Towards a physical internet: Meeting the global logistics sustainability grand challenge, Logist. Res. 3 (2011) 71—87.
[2] A. Pal, K. Kant, Internet of perishable logistics: Building smart fresh food supply chain networks, IEEE Access 7 (2019) 17675–17695.
[3] Maximizing delivered shelf-life in the end-to-end fresh food supply chain, 2016, https://www.zestlabs.com/wp-content/uploads/2016/03/Pallet-Monitoring-for-the-Fresh-Food-Supply-Chain.pdf, Last accessed 2nd April 2022.
[4] A. Pal, K. Kant, NFMI: Near field magnetic induction based communication, Comput. Netw. 181 (2020) 107548.
[5] D. Gunders, Wasted: How america is losing up to 40 percent of its food from farm to fork to landfill, 2012.
[6] How ugly fruits and vegetables can help solve world hunger, 2022, http://www.nationalgeographic.com/magazine/2016/03/global-food-waste-statistics/, Last accessed 2nd April 2022.
[7] R. Leuschner, C. Carter, T. Goldsby, Z. Rogers, Third-party logistics: A meta-analytic review and investigation of its impact on performance, J. Supply Chain Manage. 50 (1) (2014) 21–43.
[8] A. Pal, K. Kant, F2π: A physical internet architecture for fresh food distribution networks, in: IPIC, 2016.
[9] G. Fuertes, I. Soto, R. Carrasco, M. Vargas, J. Sabattin, C. Lagos, Intelligent packaging systems: Sensors and nanosensors to monitor food quality and safety, J. Sensors 2016 (2016) 4046061:1–4046061:8.
[10] L. da Costa Silva, A. Salgado, K. Pereira, V. dos Santos, Biosensors for Contaminants Monitoring in Food and Environment for Human and Environmental Health, INTECH Open Access Publisher, 2013, URL https://books.google.com/books?id=qTaKoAEACAAJ.
[11] A. Pal, K. Kant, IoT-based sensing and communications infrastructure for the fresh food supply chain, IEEE Comput. 51 (2) (2018) 76–80.

[12] A. Pal, K. Kant, Magnetic induction based sensing and localization for fresh food logistics, in: IEEE LCN, 2017, pp. 383–391.
[13] C_2Sense, 2022, http://www.c2sense.com, Last accessed 2nd April 2022.
[14] Keeping food safe from farm to fork, 2010, http://www.israel21c.org/keeping-food-safe-from-farm-to-fork/, Last accessed 2nd April 2022.
[15] Salmonella sensing system: New approach to detecting food contamination enables real-time testing, 2022, http://phys.org/news/2013-10-salmonella-approach-food-contamination-enables.html, Last accessed 2nd April 2022.
[16] M.C. do Nascimento Nunes, M. Nicometo, J.P. Emond, R.B. Melis, I. Uysal, Improvement in fresh fruit and vegetable logistics quality: berry logistics field studies, Philos. Trans. R. Soc. 372 (2017) (2014).
[17] R. Jedermann, T. Pötsch, C. Lloyd, Communication techniques and challenges for wireless food quality monitoring, Philos. Trans. R. Soc. 372 (2017) (2014) 20130304.
[18] I. Dove, Analysis of radio propagation inside the human body for in-body localization purposes, 2014, http://essay.utwente.nl/66071/, Last accessed 2nd April 2022.
[19] D. Werber, A. Schwentner, E.M. Biebl, Investigation of RF transmission properties of human tissues, 2006.
[20] H.-Z.T. Chen, A.S.-L. Lou, A study of RF power attenuation in bio-tissues, 24 (3) (2004) 141–146.
[21] E.J. Mitcham, C.H. Crisosto, A.A. Kader, Strawberry: Recommendations for maintaining postharvest quality, 2022, http://postharvest.ucdavis.edu/Commodity_Resources/Fact_Sheets/Datastores/Fruit_English/?uid=58&ds=798, Last accessed 2nd April 2022.
[22] G.E. Santagati, T. Melodia, L. Galluccio, S. Palazzo, Ultrasonic networking for E-health applications, IEEE Wirel. Commun. 20 (4) (2013).
[23] M. Masihpour, D. Franklin, M. Abolhasan, Multihop relay techniques for communication range extension in near-field magnetic induction communication systems, J. Netw. 8 (5) (2013) 999–1011.
[24] C. Bunszel, Magnetic induction: A low-power wireless alternative, 2022, http://www.usmicrowaves.com/files/papers/RF_DESIGN/34_magnetic_induction_a_low_power_wireless_alternative.pdf, Last accessed 2nd April 2022.
[25] W. Lee, J. Jeon, S. Park, Micro-modem for short-range underwater communication systems, in: Oceans, 2014.
[26] B. Benson, Y. Li, R. Kastner, B. Faunce, K. Domond, D. Kimball, C. Schurgers, Design of a low-cost, underwater acoustic modem for short-range sensor networks, in: OCEANS, 2010.
[27] D. Wei, S.S. Soto, J. Garcia, A.T. Becker, L. Wang, M. Pan, ROV assisted magnetic induction communication field tests in underwater environments, in: WUWNet, 2018, pp. 20:1–20:5.
[28] G. Wilhelm, C. Jaskolski, E. Berkenpas, Magnetic communication through metal barriers, 2008, https://patents.google.com/patent/US20080070499A1/en#patentCitations.
[29] Attenuation constant, 2022, https://itis.swiss/virtual-population/tissue-properties/database/acoustic-properties/attenuation-constant/, Last accessed 2nd April 2022.
[30] I.F. Akyildiz, P. Wang, Z. Sun, Realizing underwater communication through magnetic induction, IEEE Commun. Mag. 53 (11) (2015) 42–48.
[31] Z. Sun, I.F. Akyildiz, Magnetic induction communications for wireless underground sensor networks, IEEE Trans. Antennas and Propagation 58 (7) (2010) 2426–2435.
[32] H. Guo, Z. Sun, P. Wang, Channel modeling of MI underwater communication using tri-directional coil antenna, in: IEEE GLOBECOM, 2015, pp. 1–6.
[33] C.A. Balanis, Antenna Theory: Analysis and Design, Wiley-Interscience, 2005.
[34] X. Tan, Z. Sun, Environment-aware indoor localization using magnetic induction, in: IEEE GLOBECOM, 2015, pp. 1–6.
[35] X. Tan, Z. Sun, P. Wang, On localization for magnetic induction-based wireless sensor networks in pipeline environments, in: IEEE ICC, 2015, pp. 2780–2785.
[36] S. Gold, A. Rangarajan, A graduated assignment algorithm for graph matching, IEEE Trans. Pattern Anal. Mach. Intell. 18 (4) (1996) 377–388.
[37] H.W. Kuhn, The hungarian method for the assignment problem, Nav. Res. Logist. Q. 2 (1955) 83–97.
[38] K. O'Donoghue, P. Cantillon-Murphy, Planar magnetic shielding for use with electromagnetic tracking systems, IEEE Trans. Magn. 51 (2) (2015) 1–12.
[39] Embware development board, 2022, https://www.amazon.in/Embware-2148-Development-Board-Green/dp/B07785VF7K, Last accessed 2nd April 2022.
[40] Freelinc, 2022, http://www.freelinc.com/, Last accessed 2nd April 2022.
[41] Water amounts in fruits and vegetables, 2022, https://urbanwormcompany.com/wp-content/uploads/2018/09/Water-Amounts-in-Fruits-and-Vegetables-Handout-Week-10.pdf, Last accessed 2nd April 2022.
[42] Water in meat and poultry, 2022, https://www.fsis.usda.gov/wps/portal/fsis/topics/food-safety-education/get-answers/food-safety-fact-sheets/meat-preparation/water-in-meat-and-poultry/ct_index, Last accessed 2nd April 2022.
[43] A. Pal, K. Kant, NFMI: Connectivity for short-range IoT applications, Computer 52 (2) (2019) 63–67.
[44] R. Bansal, Near-field magnetic communication, IEEE Antennas Propag. Mag. 46 (2) (2004) 114–115.
[45] R.R.A. Syms, I.R. Young, L. Solymar, Low-loss magneto-inductive waveguides, J. Phys. D: Appl. Phys. 39 (18) (2006) 3945–3951.
[46] Z. Sun, I.F. Akyildiz, Magnetic induction communications for wireless underground sensor networks, IEEE Trans. Antennas and Propagation 58 (7) (2010) 2426–2435.
[47] H. Guo, Z. Sun, P. Wang, On reliability of underwater magnetic induction communications with tri-axis coils, in: IEEE ICC, 2019, pp. 1–6.
[48] Y. Li, S. Wang, C. Jin, Y. Zhang, T. Jiang, A survey of underwater magnetic induction communications: Fundamental issues, recent advances, and challenges, IEEE Commun. Surv. Tutor. 21 (3) (2019) 2466–2487.
[49] S. Lin, I.F. Akyildiz, P. Wang, Z. Sun, Distributed cross-layer protocol design for magnetic induction communication in wireless underground sensor networks, IEEE Trans. Wirel. Commun. 14 (7) (2015) 4006–4019.
[50] S. Kisseleff, I.F. Akyildiz, W.H. Gerstacker, Survey on advances in magnetic induction-based wireless underground sensor networks, IEEE Internet Things J. 5 (6) (2018) 4843–4856.
[51] A. Markham, N. Trigoni, Magneto-inductive networked rescue system (MINERS): Taking sensor networks underground, in: IPSN, 2012, pp. 317–328.
[52] A. Markham, N. Trigoni, S.A. Ellwood, D.W. Macdonald, Revealing the hidden lives of underground animals using magneto-inductive tracking, in: SenSys, 2010, pp. 281–294.
[53] Z. Sun, P. Wang, M.C. Vuran, M. Al-Rodhaan, A. Al-Dhelaan, I.F. Akyildiz, MISE-PIPE: Magnetic induction-based wireless sensor networks for underground pipeline monitoring, Ad Hoc Netw. 9 (3) (2011) 218–227.
[54] J. Park, P.P. Mercier, Magnetic human body communication, in: IEEE EMBC, 2015, pp. 1841–1844.
[55] H. Kim, H. Hirayama, S. Kim, K.J. Han, R. Zhang, J. Choi, Review of near-field wireless power and communication for biomedical applications, IEEE Access 5 (2017) 21264–21285.
[56] IEEE, Standard for Long Wavelength Wireless Network Protocol, IEEE Std 1902.1-2009, IEEE, 2009, pp. 1–25.
[57] X. Tan, Z. Sun, Environment-aware indoor localization using magnetic induction, in: 2015 IEEE Global Communications Conference (GLOBECOM), IEEE, 2015, pp. 1–6.
[58] T.E. Abrudan, Z. Xiao, A. Markham, N. Trigoni, Underground incrementally deployed magneto-inductive 3-D positioning network, IEEE Trans. Geosci. Remote Sens. 54 (8) (2016) 4376–4391.
[59] S. Lin, A.A. Alshehri, P. Wang, I.F. Akyildiz, Magnetic induction-based localization in randomly deployed wireless underground sensor networks, IEEE Internet Things J. 4 (5) (2017) 1454–1465.
[60] X. Tan, Z. Sun, P. Wang, On localization for magnetic induction-based wireless sensor networks in pipeline environments, in: 2015 IEEE International Conference on Communications (ICC), IEEE, 2015, pp. 2780–2785.

[61] T.E. Abrudan, Z. Xiao, A. Markham, N. Trigoni, Distortion rejecting magneto-inductive three-dimensional localization (MagLoc), IEEE J. Sel. Areas Commun. 33 (11) (2015) 2404–2417.
[62] J. Bachrach, C. Taylor, Localization in sensor networks, in: Handbook of Sensor Networks, John Wiley & Sons, Ltd, 2005, pp. 277–310, Ch. 9.
[63] A. Pal, Localization algorithms in wireless sensor networks: Current approaches and future challenges, Netw. Protoc. Algorithms 2 (1) (2010) 45–73.
[64] G. Han, H. Xu, T.Q. Duong, J. Jiang, T. Hara, Localization algorithms of wireless sensor networks: a survey, Telecommun. Syst. 52 (4) (2013) 2419–2436.
[65] N. Chuku, A. Nasipuri, Performance evaluation of an RSSI based localization scheme for wireless sensor networks to mitigate shadowing effects, in: IEEE WCNC, 2014, pp. 3124–3129.
[66] N. Chuku, A. Pal, A. Nasipuri, An RSSI based localization scheme for wireless sensor networks to mitigate shadowing effects, in: IEEE Southeastcon, 2013, pp. 1–6.
[67] B. Xu, G. Sun, R. Yu, Z. Yang, High-accuracy TDOA-based localization without time synchronization, IEEE Trans. Parallel Distrib. Syst. 24 (8) (2013) 1567–1576.
[68] Y. Wang, K.C. Ho, TDOA source localization in the presence of synchronization clock bias and sensor position errors, IEEE Trans. Signal Process. 61 (18) (2013) 4532–4544.
[69] D. Niculescu, B. Nath, Ad hoc positioning system (APS) using AOA, in: IEEE INFOCOM, Vol. 3, 2003, pp. 1734–1743.
[70] H.C. Chen, T.H. Lin, H.T. Kung, C.K. Lin, Y. Gwon, Determining RF angle of arrival using COTS antenna arrays: A field evaluation, in: IEEE MILCOM, 2012, pp. 1–6.
[71] Z. Guo, L. Min, H. Li, W. Wu, Improved DV-hop localization algorithm based on RSSI value and hop correction, Adv. Wirel. Sensor Netw. (2013) 97–102.
[72] D. Niculescu, B. Nath, DV based positioning in ad hoc networks, Telecommun. Syst. 22 (1) (2003) 267–280.
[73] F. Yu, Q. Wang, X.T. Zhang, C. Li, A localization algorithm for WSN based on characteristics of power attenuation, in: WiCOM, 2008, pp. 1–5.
[74] X. Sheng, Y. hen Hu, Maximum likelihood wireless sensor network source localization using acoustic signal energy measurements, IEEE Trans. Signal Process. (2003).
[75] L. Lazos, R. Poovendran, HiRLoc: high-resolution robust localization for wireless sensor networks, IEEE J. Sel. Areas Commun. 24 (2) (2006) 233–246.
[76] T. He, C. Huang, B.M. Blum, J.A. Stankovic, T. Abdelzaher, Range-free localization schemes for large scale sensor networks, in: ACM MobiCom, 2003, pp. 81–95.
[77] A. Singh, D. Lantigua, A. Meka, S. Taing, M. Pandher, G. Camci-Unal, Paper based sensors: emerging themes and applications, Sensors 18 (9) (2018) 2838.
[78] F. Mustafa, S. Andreescu, Chemical and biological sensors for food-quality monitoring and smart packaging, Foods 7 (10) (2018) 168.